Bioorganic & Medicinal Chemistry Letters 24 (2014) 4254–4259

Contents lists available at ScienceDirect

Bioorganic & Medicinal Chemistry Letters

journal homepage: www.elsevier.com/locate/bmcl

Synthesis and structure–activity relationship of non-peptidic antagonists of neuropilin-1 receptor

Wang-Qing Liu [a], Valentino Megale [b], Lucia Borriello [a,b,c], Bertrand Leforban [a,c], Matthieu Montès [d], Elodie Goldwaser [b,c], Nohad Gresh [a,b], Jean-Philip Piquemal [e], Reda Hadj-Slimane [c], Olivier Hermine [f,g,h], Christiane Garbay [a,b], Françoise Raynaud [a,b], Yves Lepelletier [f,g,h,*], Luc Demange [a,b,i,*]

[a] INSERM U648, Laboratory of Molecular and Cellular Pharmacochemistry, Université Paris Descartes, Sorbonne Paris Cité, UFR Biomédicale des Saints Pères, 45 rue des Saints Pères, 75270 Paris cedex 06, France
[b] Laboratoire de Chimie et Biochimie Pharmacologiques et Toxicologiques (LCBPT), UMR 8601 CNRS, Université Paris Descartes, Sorbonne Paris Cité, UFR Biomédicale des Saints Pères, 45 rue des Saints Pères, 75270 Paris cedex 06, France
[c] Tragex Pharma, 29 Rue Marcel Dassault, 92100 Boulogne-Billancourt, France
[d] Conservatoire National des Arts et Métiers, Chaire de Bioinformatique, Laboratoire Génomique, Bioinformatique et Applications, EA 4627, 292 rue Saint Martin, 75003 Paris, France
[e] Laboratoire de Chimie Théorique, Sorbonne Universités, UPMC, Paris 6, case courrier 137, 4, place Jussieu, 75252 Paris, France
[f] INSERM UMR 1163, Laboratory of Cellular and Molecular Basis of Normal Hematopoiesis and Hematological Disorders, 24 Boulevard Montparnasse, 75015 Paris, France
[g] Paris Descartes University-Sorbonne Paris Cité, Imagine Institute, 24 boulevard Montparnasse, 75015 Paris, France
[h] CNRS ERL 8254, 24 Boulevard Montparnasse, 75015 Paris, France
[i] Institut de Chimie de Nice (ICN), UMR 7272 CNRS, Université de Nice Sophia Antipolis, Parc Valrose, 06108 Nice cedex 1, France

ARTICLE INFO

Article history:
Received 11 June 2014
Revised 9 July 2014
Accepted 10 July 2014
Available online 17 July 2014

Keywords:
Angiogenesis
Neuropilin
Protein–protein interaction
Docking to receptor
Heterocycles

ABSTRACT

Neuropilins (NRPs) are VEGF-A_{165} co-receptors over-expressed in tumor cells, and considered as targets in angiogenic-related pathologies. We previously identified compound **1**, the first non-peptidic antagonist of the VEGF-A_{165}/NRP binding, which exhibits in vivo anti-angiogenic and anti-tumor activities. We report here the synthesis and biological evaluations of new antagonists structurally-related to compound **1**. Among these molecules, **4a**, **4c** and **4d** show cytotoxic effects on HUVEC and MDA-MB-31 cells, and antagonize VEGF-A_{165}/NRP-1 binding. This study confirmed our key structure–activity relationships hypothesis and paved the way to compound **1** 'hit to lead' optimization.

Angiogenesis plays a critical role in several diseases such as cancer,[1] arthritis[2,3] or retinopathies.[4] Among the pro-angiogenic factors, VEGF-A_{165}, a spliced form of VEGF-A (Vascular Endothelial Growth Factor), is considered as one of the most efficient, and its over-expression has been observed in tumor angiogenesis.[5] Basically, VEGF-A_{165} binds structurally related tyrosine kinase receptors located on the endothelial cells (VEGF-R1 (Flt-1), VEGF-R2 (Flk-2) and VEGF-R3) and two co-receptors, lacking cytosolic catalytic activity: neuropilins 1 and 2 (NRPs).[6,7] Neuropilins are 120–130 kDa transmembrane glycoproteins, initially described as mediators for neuronal guidance, and two homologs (NRP-1 and NRP-2, which share 44% amino acid sequence identity and identical domain structures) have been described.[8,9] NRPs form ternary complex with VEGFRs and VEGF-A_{165} and so modulate the angiogenesis signaling pathways.[6] Moreover, in cancers, NRPs over-expression enhances tumor growth and invasion which are associated with a poor prognosis.[10–15] Consequently, NRPs might be considered as potential targets in the treatment of angiogenesis-related diseases.[16]

The use of small organic molecules as antagonists for the protein–protein interaction between VEGF-A_{165} and NRPs is an innovative way to develop anti-angiogenic drugs. To date, at the best of our knowledge, no VEGF-A_{165}/NRP antagonist has reached clinics, but two pseudo-peptides approaches have been developed (Chart 1). Firstly, Barberi-Heyob and co-workers used a heptapeptide (ATWLPPR) to design a sugar-based peptidomimetic antagonist exhibiting an IC_{50} in the 90 μM range.[17,18] Secondly, Zachary's group designed two antagonists based upon the tetrapeptide TKPR, also called tuftsin, mimicking the C-terminal tail of VEGF-A_{165}. Thus, the bicyclic peptide EG3287 and the pseudo-peptide EG00229 have been described.[19,20] They exhibit potencies of

* Corresponding authors. Tel.: +33 (0)1 42 75 42 83 (Y.L.), +33 (0)4 92 07 65 96 (L.D.).
E-mail addresses: y.lepelletier@gmail.com (Y. Lepelletier), luc.demange@parisdescartes.fr (L. Demange).

http://dx.doi.org/10.1016/j.bmcl.2014.07.028
0960-894X/

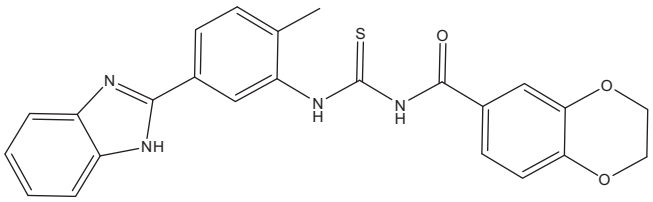

Compound **1**

Chart 1. Structure of compound **1**.

respectively $K_I = 1.2\ \mu M$ and $IC_{50} = 8\ \mu M$ (measured with ^{125}I-VEGF-A_{165} and porcine aortic endothelial cells expressing NRP-1). In addition, EG00229 reduces the viability of human lung carcinoma A549 cells and strengthens the potency of paclitaxel.[20] Nevertheless, pseudo-peptidic compounds rarely provide pharmacological agents, and therefore we focused our efforts on the identification of new VEGF-A_{165}/NRP-1 non-peptidic antagonists.

By an in silico/in vitro screening procedure, our team reported recently the very first and original fully non-peptidic VEGF-A_{165}/NRP antagonist (compound **1**, chart 1).[21] In vitro, this 'hit' bound NRP-1 and NRP-2 with IC_{50} in the micromolar range and exhibited anti-angiogenic and pro-apoptotic activities in cellular assays. Moreover, in vivo studies on MDA-MB-231 NOG-xenografted mice pointed out that compound **1** increased animal survival and reduced cell tumor growth. Its in vivo anti-angiogenic and pro-apoptotic potencies were also demonstrated by CD34, CD31 and Ki-67 immunostaining.[21]

The structure of compound **1** might be divided into four sections: a benzimidazole core connected to a methylbenzene linked to a benzodioxane motif through an unusual carboxythiourea spacer. Taking advantage of the known X-ray structure of tuftsin bound to NRP-1, compound **1** was docked in the NRP-1 extracellular b1 coagulation factor domain, and in the tuftsin arginine binding pocket.[22,23] This docking, performed using ICM-version-3.4[24] suggested that compound **1** acts as a staple and pointed out that the benzimidazole core mimics an arginine guanidinium, in order to respect the N-terminal arginine rule.[21] We next performed preliminary energy-minimization studies using the Accelrys software[25] and the CFF91 force-field. Two interesting energy-minima candidates were found.

In the first minimized case (Fig. 1A), the benzimidazole is stacked in parallel between Tyr-353 and Tyr-297 and in a perpendicular fashion to Trp-301. Its N–H is engaged in an H-bond with the Asp-320 carboxylate. The carboxythiourea entity binds to Lys-351 through H-bonds involving both its carbonyl and thiocarbonyl groups. The Tyr-353 hydroxyl proton appears to interact with the electron-rich ring of the benzene of benzodioxane, while the hydroxyl proton of Tyr-297 appears to interact with the electron-rich methylbenzene ring. The dioxane ring is partially stacked over the methyl group of Thr-413. The benzene ring of benzodioxane is stacked perpendicular to methylbenzene and benzimidazole. The overall conformation of the hit is stabilized by a hammer-like stacking interaction of the benzene ring of benzimidazole over the aromatic ring of the methylbenzene.

In the second minimized case (Fig. 1B), the benzimidazole core is again stacked in a parallel fashion between Tyr-297 and Tyr-353 and is perpendicular to Trp-301. Asp-320 now interacts with the partly acidic C–H hydrogen of the benzimidazole benzene instead of the benzimidazole N–H. The thiocarbonyl sulfur accepts a proton from the N–H indole of Trp-301, while the carbonyl oxygen is involved in an intramolecular H-bond with the thiocarbonyl N–H group.

In order to select one of these two structure–activity relationship hypotheses, we report here synthesis and biological evaluations of new antagonists structurally related to compound **1**. Thus, compound **1** and its derivatives **4a**–**n**, which encompass structural modifications in the benzimidazole and/or the phenolic and/or the benzodioxane moieties, are synthesized using a convergent procedure (Scheme 1). On one hand, the reductive condensation of substituted *o*-phenylenediamine ($X = NH_2$) with 4-methyl-3-nitrobenzaldehyde or 3-nitrobenzaldehyde in presence of sodium metabisulfite in refluxing DMF afforded an aminophenylbenzimidazole (**2**) with a 50–65% yield.[26–28] Interestingly, following the same synthetic route, benzothiazole is obtained using 2-aminobenzenethiol (X = SH) as the starting material with a 50% yield.[28] On the other hand, different acyl isothiocyanates (**3**) are quantitatively prepared from corresponding carboxylic acids in two steps through acyl chloride and subsequent thiocyanate substitution.[29] Lastly, the nucleophilic addition of aminophenylbenzimidazoles (**2**) to acyl isothiocyanates (**3**) in refluxing dry acetone leads to compound **1** and its derivatives **4a**–**n** with an average 45% yield (scheme 1).[29]

The newly synthesized antagonists were firstly evaluated on endothelial cells (HUVEC) and on breast invasive tumor cells (MDA-MB-231). Cell adhesion was evaluated by a colorimetric test using cristal violet adhesion,[30] while cytotoxicity assays (cell viability) were based on tetrazolium salt cleavage by viable cells.[31] They were performed after three days of cell incubation at 37 °C with various concentrations of each antagonist. The results are given as IC_{50} values and are reported in Table 1. In a second step, eight molecules were evaluated as antagonists of the biotinylated (bt)-VEGF-A_{165}/NRP-1 and/or (bt)-VEGF-A_{165}/VEGF-R1 binding as control at the unique concentration of 10 μM by a binding assay.[32] The percentage of displaced (bt)-VEGF-A_{165} by the compounds are shown in Table 2.

Cellular assays demonstrate a good correlation between results obtained on cell adhesion and cytotoxicity. In terms of selectivity, the newly synthesized molecules seem to be more potent against HUVEC than against MDA-MB-231 breast cancer cells (e.g., **4d** reduced viability/proliferation of HUVEC twenty times higher than the same assay results obtained for MDA-MB-231). Moreover, **4a**, **4c** and **4d** are more selective than compound **1** in the cytotoxic assay for HUVEC, which has a stronger ability for angiogenesis, compared to MDA-MB-231 cells.

Compounds **1**, **4a**, **4c**,**d** show sub-micromolar cellular activities on HUVEC, and antagonize at 10 μM significantly the (bt)-VEGF-A_{165} binding to NRP-1. These results confirm that the removal of the methyl group of the benzene (**4a**, **4d**) and the substitution of the dioxane ring by a dioxolane ring are not detrimental in terms of NRP-1-b1 binding (**4a** and **4d** respective binding inhibition at 10 μM are 38 ± 2% and 46 ± 3% compared to 34 ± 3% for **1**). Moreover, **4a** and **4d** show a rather good selectivity for NRP-1, since they are respectively three and seven times more potent to antagonize (bt)-VEGF-A_{165}/NRP-1 than the (bt)-VEGF-A_{165}/VEGF-R1 interaction (shown in Table 2).

Conversely, compounds in which the benzimidazole ring was switched into a benzothiazole exhibited some lower cellular activity and also lower receptor binding affinity (**4m**). Thus, the most potent benzothiazole derivative, compound **4m**, showed three-fold lower activity against HUVEC proliferation when compared to **4d** ($IC_{50} = 0.9 \pm 0.03\ \mu M$) and it partly antagonized (bt)-VEGF-A_{165} binding to NRP-1 (14 ± 1%). According to the docking hypothesis,[21] the benzimidazole ring is deeply inserted into the arginine binding pocket and mimics the arginine guanidinium motif in order to fulfill the NRPs binding C-end rule.[33] These results demonstrated the structural relevance of the benzimidazole nitrogen H-bond donor, missing in the benzothiazole ring. This appeared to be very detrimental in terms of receptor binding. Consequently, it might be suggested that the first energy-minimization model (Fig. 1A) might be more accurate than the second (Fig. 1B).

Finally, the introduction of a substituent in the benzimidazole ring (even a fluorine, **4f**, yet a small atom known to increase global

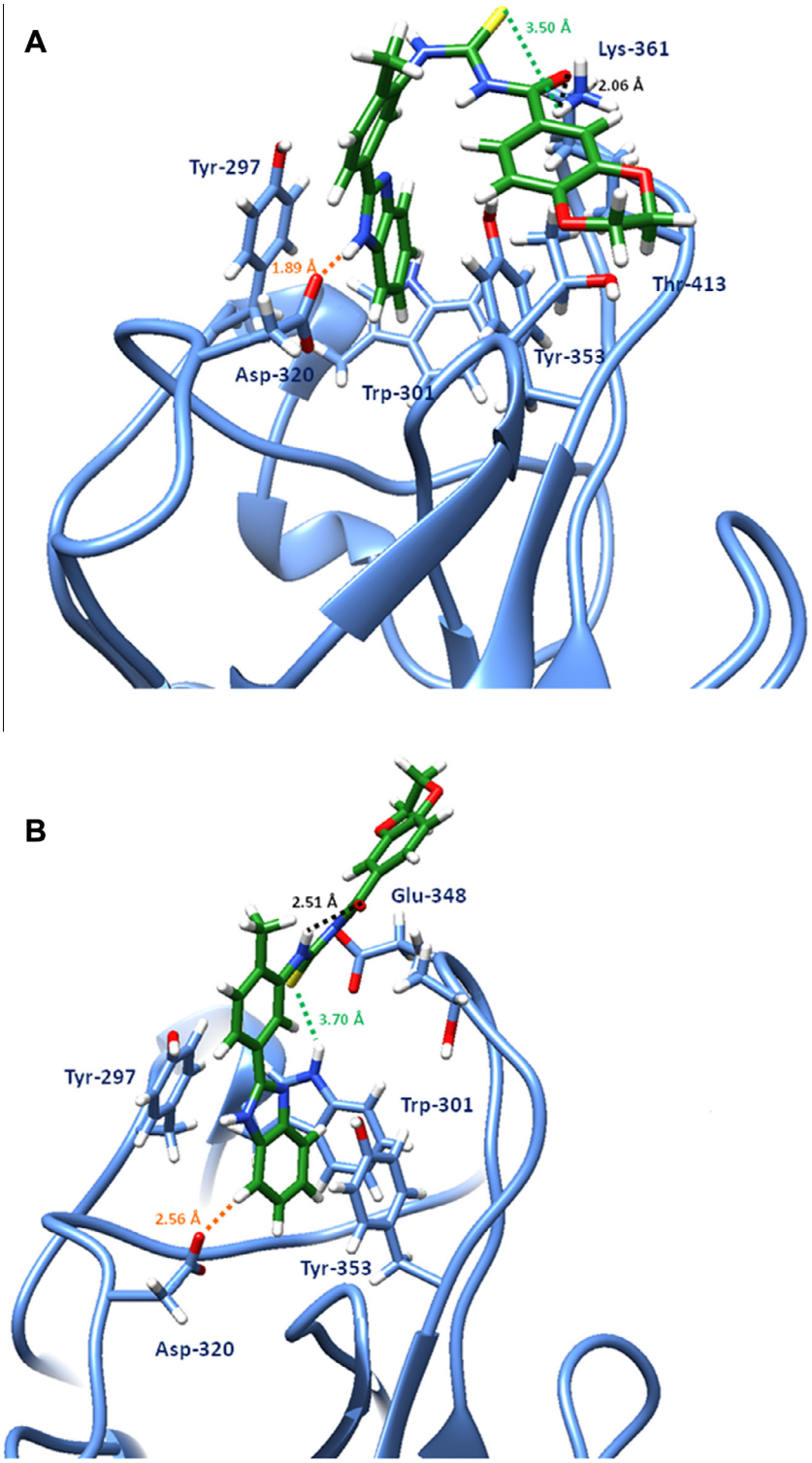

Figure 1. Two docking hypotheses A and B for compound **1** in the NRP-1 b1 domain (see text for more details). The hydrogen bonds network between the antagonist and NRP-1 is outlined as orange, green and black dashed lines. H-bond lengths are also specified.

molecule hydrophobicity)[34,35] is detrimental, probably due to enhancement of the steric hindrance. The opening (**4g–i**) or the suppression (**4j**,**k**) of the dioxane ring is also very disadvantageous in terms of cellular activity. Surprisingly, although **4e** and **4g** retain binding capacity for NRP-1, their cellular activity is decreased.

We then turned our attention on the relevance of the linker's structure and therefore synthesized molecules with a partly reduced and more flexible linker (**7a**,**b**) encompassing a carboxyurea motif (**9**) (Scheme 2). These compounds are synthesized following the same synthetic route as for **1** and **4a–n**. According with the two step conversion of primary amine to isothiocyanate described by Munch and co-workers, commercial benzo[*d*][1,3]dioxol-5-ylmethanamine is treated with a mixture of carbon disulfide, triethylamine and di-*tert*butyldicarbonate in presence of a catalytic amount of DMAP to afford quantitatively isocyanate **6**.[36] The subsequent condensation of **6** with **2** in

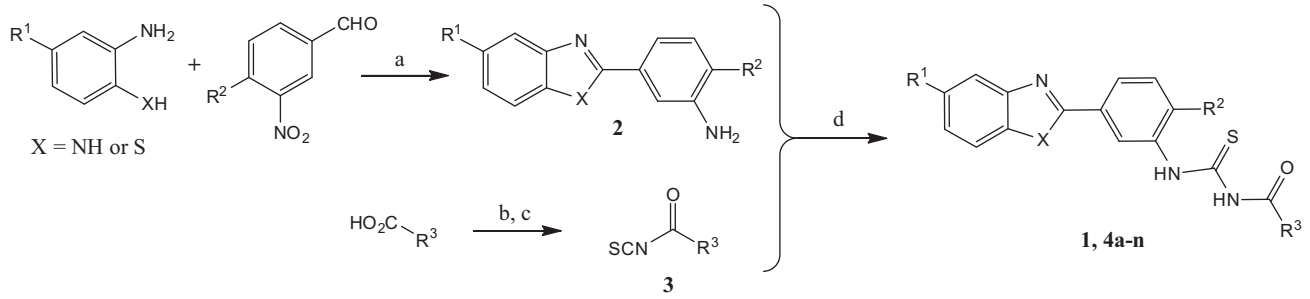

Scheme 1. Synthetic route to compound **1** and its derivatives **4a**–**n**. Reagents and conditions: (a) $Na_2S_2O_5$ 3 equiv, refluxing DMF, 3 h; (b) refluxing $SOCl_2$, 2 h; (c) $NH_4^+NCS^-$, refluxing dry acetone, 2 h; (d) refluxing dry acetone, 1 h. Final products are purified by crystallization in ethanol.

Table 1
Cellular effects of newly synthesized antagonists[30,31]

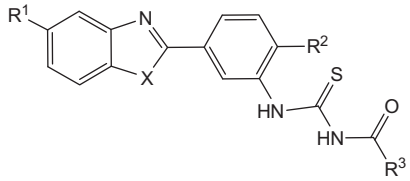

Compd	X	R^1	R^2	R^3	IC_{50} HUVEC (μM)		IC_{50} MDA-MB-231 (μM)	
					Adhesion	Cytotoxicity	Adhesion	Cytotoxicity
1	NH	H	CH_3	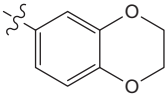	0.15 ± 0.02	0.24 ± 0.02	0.50 ± 0.05	0.53 ± 0.07
4a	NH	H	H		<0.1	0.05 ± 0.01	0.50 ± 0.12	0.40 ± 0.20
4b	NH	CN	H		Nd.	1	Nd.	>10
4c	NH	H	CH_3	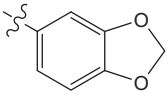	0.75 ± 0.05	1.5 ± 0.5	6.0 ± 2.0	6.0 ± 2.0
4d	NH	H	H		0.3 ± 0.1	0.3 ± 0.1	6.0 ± 2.0	6.0 ± 2.0
4e	NH	CN	H		6.0 ± 2.0	Nd.	Nd.	Nd.
4f	NH	F	CH_3		>10	>10	Nd.	Nd.
4g	NH	H	H	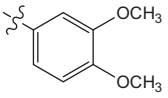	5	6	10	>10
4h	NH	H	CH_3	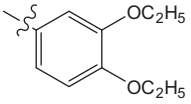	6	Nd.	Nd.	Nd.
4i	NH	H	H		8	8	Nd.	Nd.
4j	NH	H	H	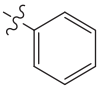	>10	>10	>10	>10
4k	NH	H	CH_3		>10	>10	>10	>10
4l	S	H	H	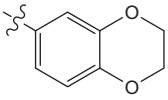	2.6 ± 0.3	2.6 ± 0.3	>10	>10
4m	S	H	H	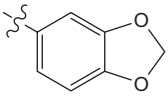	0.90 ± 0.03	1	8	10
4n	S	H	CH_3		5.0 ± 0.25	5.0 ± 0.25	>10	>10

Compounds **4a**–**n** were tested at various concentrations. IC_{50} values, calculated from the dose–response curves, are reported in μM. Nd.: not determined. IC_{50} values reported as >10 indicate that the compounds did not display any inhibitory activity at the highest concentration tested (10 μM).

refluxing dry acetone leads to compounds **7a**,**b** (20% yield). Lastly, the carboxyisocyanate **8** is obtained from the corresponding carboxylic acid in two steps using sodium isocyanate in presence of a catalytic amount of $SnCl_4$.[37] Its subsequent condensation with phenylbenzimidazole **2** leads to the required product **9**.

These molecules were evaluated for cell adhesion and cytotoxicity, and results are summarized in Table 3. It appears clearly that the carbonyl's reduction (compounds **7a**,**b**) and the subsequent increase of the linker's flexibility induced a dramatic loss of efficiency for both cellular assays (IC_{50} >10 μM). Conversely, compound **9** retained a significant cytotoxic effect on HUVEC (IC_{50} = 8 μM). This result might be correlated with the first docking hypothesis (Fig. 1A), in which the linker's oxygen seems to be close to the ε-amine of Lys-351 (2.06 Å), and therefore might be involved in an H-bond. The maintenance of this H-bonding in compound **9** might explain its significant cellular activity. In addition, these

Table 2
Antagonist effects of the newly synthesized compound on VEGF-A_{165} binding to NRP and VEGF-R1[32]

Compd	Binding inhibition of VEGF-A_{165} at 10 μM (%)	
	NRP-1	VEGF-R1
1	34 ± 3	18 ± 3
4a	38 ± 2	7 ± 4
4b	0 ± 0	11 ± 5
4d	46 ± 3	7 ± 3
4e	37 ± 3	Nd.
4h	32 ± 1	22 ± 3
4i	14 ± 3	Nd.
4m	14 ± 1	13 ± 1

Compounds were tested at the unique concentration of 10 μM, and antagonist activity was determined through a chemoluminescent assay. Nd.: not determined.

results underlie the structural relevance of the linker conjugation that induces rigidity and flatness to the carboxythiourea motif.

Concerning this latter observation, quantum chemistry calculations have unraveled the stringent conformational requirements of the linker due to its polyconjugation. We have thus quantified the variations of the linker conformational energies upon performing 15 degree stepwise torsions around its successive N–C(S), C(S)–N, and N–C(O) bonds. Even limited departures from planarity, starting around 40 degrees, entailed steep raises of the conformational energy, of 5 kcal/mol and above.[38] Disrupting conjugation effects of the linker, as occurs in inactive derivatives (**7a**,**b**), could relax the energy barriers but result into 'floppier' compounds with looser conformational properties. Binding of such compounds to NRP-1 could entail a loss of conformational entropy, which would be detrimental in the overall energy balances.

In summary, starting from two energy-minimization hypotheses, we explored structure–activity relationship around compound **1**, the first non-peptidic NRP-1 antagonist. These results suggest that there are more stabilizing interactions in the first complex (Fig. 1A) than in the second one (Fig. 1B). This latter complex could possibly be considered as a higher-energy intermediate as compound **1** docks to its binding site to intercalate its benzimidazole ring between Tyr-297 and Tyr-353. More extensive simulations on the complexes of NRP-1 with compound **1** and its derivatives including solvation effects are planned with the SIBFA polarizable molecular mechanics/dynamics procedure[39] and will be reported

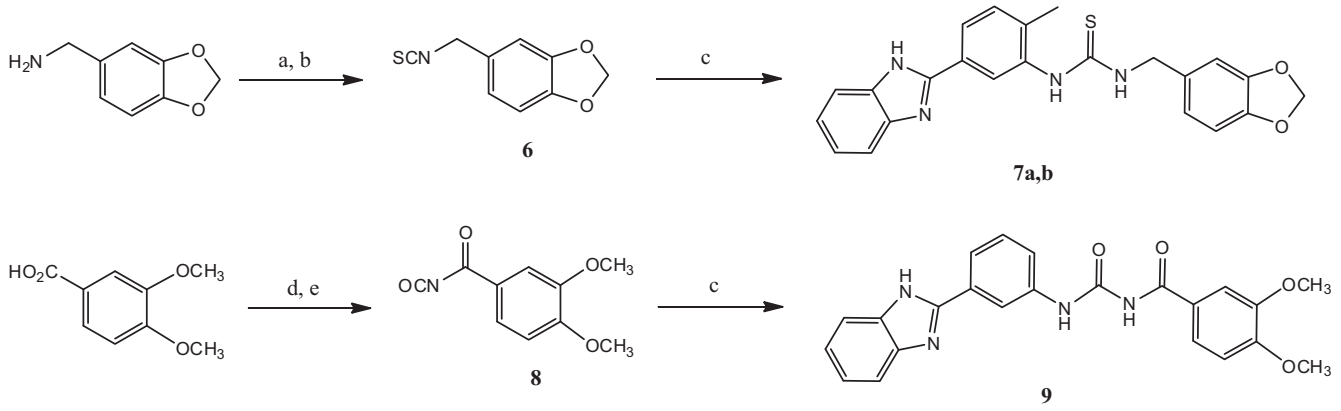

Scheme 2. Synthetic route to derivatives **7a**, **7b** and **9** encompassing structural modifications in the linker. Reagents and conditions : (a) CS_2 10 equiv, NEt_3 1 equiv, absolute ethanol, rt, 1 h; (b) Boc_2O 1 equiv, then DMAP cat., absolute ethanol, 0 °C then rt for 30 min; (c) compound **2** (X = NH, R^1 = H, R^2 = H or CH_3) 1 equiv in refluxing dry acetone, 1 h; (d) refluxing $SOCl_2$, 2 h.; (e) NaOCN 1.3 equiv, $SnCl_4$ cat. refluxing dry acetone, 2 h. Final products are purified by crystallization in ethanol.

Table 3
Cellular effect of newly synthesized antagonists[30,31]

Compd	Structure	IC_{50} HUVEC cells (μM)		IC_{50} MDA-MB-231 cells (μM)	
		Adhesion	Cytotoxicity	Adhesion	Cytotoxicity
7a	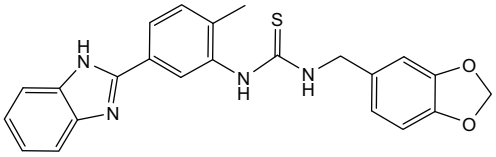	>10	>10	>10	>10
7b	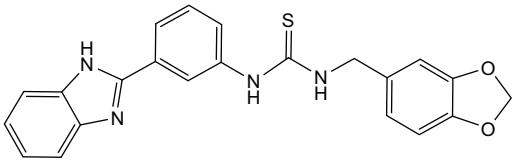	>10	>10	>10	>10
9	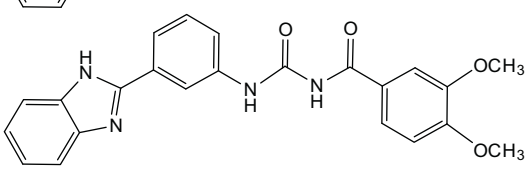	8	8	Nd.	Nd.

Compounds **7a**, **b** and **9** were tested at various concentrations. IC_{50} values, calculated from the dose–response curves, are reported in μM. Nd.: not tested. IC_{50} values reported as >10 indicate that the compounds did not display any inhibitory activity at the highest concentration tested (10 μM).

in due course. Lastly, among the newly-synthesized compounds, **4a**, **4c** and **4d**, which are structurally very close to compound **1**, might be considered as new 'hits' due to their preliminary biological evaluations. These compounds should be now structurally optimized. Finally, complementary molecular and cellular studies about **4a**, which showed in this work the most potent effects on cellular assay, are currently in progress, and should be soon reported.

Acknowledgments

This research was supported by grant from the 'Institut National du Cancer' (INCa 'Angiomed' 2007-2010 grant). L.B. and E.G. were supported by ANRT (Association Nationale de la Recherche et de la Technologie' CIFRE fellowship. V.M. was supported by 'Leonardo da Vinci project' UNIPHARMA-GRADUATES (www.unipharmagraduates.it) coordinated by Sapienza University of Rome and promoted by the Noopolis Foundation (www.noopolis.eu), Italy. Drs. Rachid Benhida and Nadine Martinet are gratefully acknowledged for the critical reading of this paper.

Supplementary data

Supplementary data associated with this article can be found, in the online version, at http://dx.doi.org/10.1016/j.bmcl.2014.07.028.

References and notes

1. Ferrara, N.; Kerbel, R. S. *Nature* **2005**, *438*, 967.
2. Walsh, D. A.; McWilliams, D. F.; Turley, M. J.; Dixon, M. R.; Fransès, R. E.; Mapp, P. I.; Wilson, D. *Rheumatology* **2010**, *49*, 1852.
3. Bonnet, C. S.; Walsh, D. A. *Rheumatology* **2005**, *44*, 7.
4. Miller, J. W.; Le Couter, J.; Strauss, E. C.; Ferrara, N. *Opthalmology* **2013**, *120*, 106.
5. Biselli-Chicotte, P. M.; Oliveira, A. R.; Pavarino, E. C.; Goloni-Bertollo, E. M. *J. Cancer Res. Clin. Oncol.* **2012**, *138*, 363.
6. Geretti, E.; Shimizu, A.; Klagsbrun, M. *Angiogenesis* **2008**, *11*, 31.
7. Grunewald, F. S.; Prota, A. E.; Giese, A.; Ballmer-Hofer, K. *Biochim. Biophys. Acta* **2010**, *1804*, 567.
8. He, Z.; Tessier-Lavigne, M. *Cell* **1997**, *90*, 739.
9. Kolodkin, A. L.; Levengood, D. V.; Rowe, E. G.; Tai, Y. T.; Giger, R. J.; Ginty, D. D. *Cell* **1997**, *90*, 753.
10. Golfinopoulos, V.; Salanti, G.; Pavlidis, N.; Ioannidis, J. P. *Lancet Oncol.* **2007**, *8*, 898.
11. Osada, H.; Tokunaga, T.; Nishi, M.; Hatanaka, H.; Abe, Y.; Tsugu, A.; Kijima, H.; Yamazaki, H.; Ueyama, Y.; Nakamura, M. *Anticancer Res.* **2004**, *24*, 547.
12. Hansel, D. E.; Wilentz, R. E.; Yeo, C. J.; Schulick, R. D.; Montgomery, E.; Maitra, A. *Am. J. Surg. Pathol.* **2004**, *28*, 347.
13. Ghosh, S.; Sullivan, C. A. W.; Zerkowski, M. P.; Molinaro, A. M.; Rimm, D. L.; Camp, R. L.; Chung, G. G. *Hum. Pathol.* **2008**, *39*, 1835.
14. Prud'homme, G. J.; Glinka, Y. *Oncotarget* **2012**, *3*, 921.
15. Wild, J. R.; Staton, C. A.; Chapple, K.; Corfe, B. M. *Int. J. Exp. Pathol.* **2012**, *93*, 81.
16. Barr, M. P.; Byrne, A. M.; Duffy, A. M.; Condron, C. M.; Devocelle, M.; Harriott, P.; Bouchier-Hayes, D. J.; Harmey, J. H. *Br. J. Cancer* **2005**, *92*, 328.
17. Starzec, A.; Ladam, P.; Vassy, R.; Badache, S.; Bouchemal, N.; Navaza, A.; DuPenhoat, C. H.; Perret, G. Y. *Peptides* **2007**, *28*, 2397.
18. Novoa, A.; Pellegrini-Moise, N.; Bechet, D.; Barberi-Heyob, M.; Chapleur, Y. *Bioorg. Med. Chem.* **2010**, *18*, 3285.
19. Jia, H.; Bagherzadeh, A.; Hartzoullakis, B.; Jarvis, A.; Lohr, M.; Shaikh, S.; Aqil, R.; Cheng, L.; Tickner, M.; Esposito, D.; Harris, R.; Driscoll, P. C.; Selwood, D. L.; Zachary, I. C. *J. Biol. Chem.* **2006**, *281*, 13493.
20. Jarvis, A.; Allerston, C. K.; Jia, H.; Herzog, B.; Garza-Garcia, A.; Winfield, N.; Ellard, K.; Aqil, R.; Lynch, R.; Chapman, C.; Hartzoulakis, B.; Nally, J.; Stewart, M.; Cheng, L.; Menon, M.; Tickner, M.; Djordjevic, S.; Driscoll, P. C.; Zachary, I.; Selwood, D. L. *J. Med. Chem.* **2010**, *53*, 2215.
21. Borriello, L.; Montès, M.; Lepelletier, Y.; Leforban, B.; Liu, W.-Q.; Demange, L.; Delhomme, B.; Pavoni, S.; Jarray, R.; Boucher, J. L.; Dufour, S.; Hermine, O.; Garbay, C.; Hadj-Slimane, R.; Raynaud, F. *Cancer Lett.* **2014**, *349*, 120.
22. Van der Kooi, C. W.; Jusino, M. A.; Perman, B.; Neau, D. B.; Bellamy, H. D.; Leahy, D. *J. Proc. Natl. Acad. Sci. U.S.A.* **2007**, *104*, 6152.
23. Zanuy, D.; Kotl, R.; Nussinov, R.; Teesalu, T.; Sugahara, K. N.; Aleman, C.; Haspel, N. *J. Struct. Biol.* **2013**, *182*, 78.
24. Abagyan, R.; Totrov, M. *J. Mol. Biol.* **1994**, *235*, 983.
25. Accelrys Inc., San Diego, CA 92121, USA.
26. Han, X.; Ma, H.; Wang, Y. *Russ. J. Org. Chem.* **2008**, *44*, 863.
27. Richards, M. L.; Lio, S. C.; Sinha, A.; Banie, H.; Thomas, R. J.; Major, M.; Tanji, M.; Sircar, J. C. *Eur. J. Med. Chem.* **2006**, *41*, 950.
28. *General procedure for benzimidazole and benzothiazole synthesis (**2**):* A solution of commercial nitrobenzaldehyde (1.0 equiv) and sodium metabisulfite (3.0 equiv) is warmed into refluxing DMF for 1 h. After cooling at room temperature, a solution of *o*-phenylenediamine (1.0 equiv) or 2-aminobenzenethiol (1.0 equiv) in DMF is carefully added. The mixture is stirred in refluxing DMF until the reaction is completed. After cooling at room temperature, the product is precipitated by addition of a frozen mixture of water and ethyl acetate (1:2). Crude material is filtrated and washed with cold ethyl acetate, then with water and finally with ether. Product is dried under vacuum and might be used for the next step without further purification.
29. *General procedure for antagonists synthesis (**1**, **4a–n**):* A mixture of commercial carboxylic acid in freshly distilled thionyl chloride is warmed into reflux for 2 h, then cooled to room temperature and evaporated under vacuum to dryness to afford quantitatively corresponding acid chlorides (**3**). This crude material might be used without further purification. A mixture of these acid chloride (1.0 equiv) and ammonium thiocyanate (1.0 equiv) is heated in refluxing dry acetone for 1 h. Then, the mixture is cooled to room temperature, and a solution of benzimidazole in dry acetone is carefully added. The mixture is warmed again for 1 h, then cooled to 0 °C, and hydrolyzed with ice. The precipitate is washed with cold water and crude material is crystallized into ethanol.
30. *General procedure for cell viability assay (crystal violet):* HUVEC and MDA-MB-231 are seeded in 96-well plate at 3×10^3 and 5×10^3 cells per well respectively, and then treated with the inhibitors at different concentrations for 72 h. Next, they were fixed in 4% paraformaldehyde for 15 min, washed in PBS pH 7.4, and stained with 0.04% crystal violet for 30 min. Then 2% Triton X-100 was added to the dried plates, and the OD at 595 nm was measured for detecting cell adhesion. The results are expressed as the mean of three independent experiments with three determinations per tested concentration and per experiment. For each compound, the IC_{50} value was determined from a sigmoid dose–response curve using Graph-Pad Prism (GraphPad Software, San Diego, CA, USA).
31. *General procedure for cytotoxicity assay (WST-1 measurement):* HUVEC and MDA-MB-231 were plated at 3×10^3 and 5×10^3 cells per well in 96-well plate respectively in 200 μL of media. Cells were treated with different compounds one day after seeding. After 48 h, the culture media was removed, then the 4-[3-(4-Iodophenyl)-2-(4-nitrophenyl)-2H-5-tetrazolio]-1,3-benzene disulfonate (WST-1) from Roche® was added, and the plates were incubated at 37 °C for 1–2 h. Optical Density (OD) was measured with a microplate reader (Bio-Rad) at 490 nm to determine the cell viability. The results are expressed as the mean of three independent experiments with three determinations per tested concentration and per experiment. For each compound, the IC_{50} value was determined from a sigmoid dose–response curve using Graph-Pad Prism (GraphPad Software, San Diego, CA, USA).
32. *General procedure for receptor binding assay:* VEGF-R1 or NRP-1 (R&D Systems, Paris, France) were coated to the surface of a 96-well plate by overnight incubation at 0.2 μg/mL in PBS at 4 °C. The plate was washed three times in PBS containing 0.5% Tween 20, after which it was treated for 2 h at 37 °C with 0.5% BSA to block non-specific binding and rinsed with PBS. The plates were then incubated with different compounds at 50 μL/well (10^{-4} M) for one hour at 37 °C followed by 2 h incubation at 37 °C with biotinylated VEGF supplemented with 4 μg/mL heparin. VEGF was added at 200 μg/mL for NRP-1 and at 100 μg/mL for VEGF-R1. Binding was detected using Streptavidin-Horseradish Peroxidase (Amersham, Pittsburgh, USA). Chemiluminescence was quantified with an EnVi-sion TM 2101 Multilabel reader (Perkin Elmer, Massachusetts, USA).
33. Teesalu, T.; Sugahara, K. N.; Kotamraju, V. R.; Ruoslahti, E. *Proc. Natl. Acad. Sci. U.S.A.* **2009**, *106*, 16157.
34. Tsukada, Y.; Iwamoto, K.; Furutani, H.; Matsushita, Y.; Abe, Y.; Matsumoto, K.; Monda, K.; Hayase, S.; Kawatsura, M.; Itoh, T. *Tetrahedron Lett.* **2006**, *47*, 1801.
35. Schlosser, M.; Michel, D. *Tetrahedron* **1996**, *52*, 99.
36. Munch, H.; Hansen, J. S.; Pittelkow, M.; Christensen, J. B.; Boas, U. *Tetrahedron Lett.* **2008**, *49*, 3117.
37. Dzeng, M.-Z.; Caubere, P. *Tetrahedron* **1988**, *44*, 6079.
38. Goldwaser, E.; DeCourcy, B.; Demange, L.; Garbay, C.; Raynaud, F.; Hadj-Slimane, R.; Piquemal, J.-P.; Gresh, N. submitted for publication.
39. Gresh, N.; Cisneros, G. A.; Darden, T. A.; Piquemal, J.-P. *J. Chem. Theory Comput.* **2007**, *3*, 1960.